

# Simulations of the reionization of the clumpy intergalactic medium with a novel particle-based two-moment radiative transfer scheme

Tsang Keung Chan<sup>1,2</sup> , Alejandro Benitez-Llambay<sup>3</sup>, Tom Theuns<sup>1,2</sup> and Carlos Frenk<sup>1,2</sup>

<sup>1</sup>Institute for Computational Cosmology, Durham University, South Road, Durham DH1 3LE, UK  
email: [tsang.k.chan@durham.ac.uk](mailto:tsang.k.chan@durham.ac.uk)

<sup>2</sup>Department of Physics, Durham University, South Road, Durham DH1 3LE, UK

<sup>3</sup> Dipartimento di Fisica G. Occhialini, Università degli Studi di Milano Bicocca, Piazza della Scienza, 3 I-20126 Milano MI, Italy

**Abstract.** The progress of cosmic reionization depends on the presence of over-dense regions that act as photon sinks. Such sinks may slow down ionization fronts as compared to a uniform intergalactic medium (IGM) by increasing the clumping factor. We present simulations of reionization in a clumpy IGM resolving even the smallest sinks. The simulations use a novel, spatially adaptive and efficient radiative transfer implementation in the SWIFT SPH code, based on the two-moment method. We find that photon sinks can increase the clumping factor by a factor of  $\sim 10$  during the first  $\sim 100$  Myrs after the passage of an ionization front. After this time, the clumping factor decreases as the smaller sinks photoevaporate. Altogether, photon sinks increase the number of photons required to reionize the Universe by a factor of  $\eta \sim 2$ , as compared to the homogeneous case. The value of  $\eta$  also depends on the emissivity of the ionizing sources.

**Keywords.** radiative transfer, cosmology:early universe, galaxies:intergalactic medium

---

## 1. Introduction

During the epoch of reionization (EoR) at redshifts  $z \gtrsim 6$ , the universe underwent a global phase transition from mostly neutral to mostly ionized due to photoionization of the intergalactic medium (IGM), most likely by hot stars in the first galaxies. This change in neutral fraction strongly affects the transmission properties of the IGM in Lyman lines and hence the detectability and observability of galaxies (see e.g. [Robertson 2021](#) for a recent review). Photoionization also increases the IGM's temperature from  $\sim 10$  K to  $\gtrsim 10^4$  K, which affects the growth of small density perturbations and suppresses the formation and growth of dwarf galaxies ([Efstathiou 1992](#); [Bullock, Kravtsov & Weinberg 2000](#)). Such suppression helps reconciling the low amplitude of the observed luminosity function of the Milky Way with the high amplitude of the subhalo mass function as inferred from simulations ([Moore \*et al.\* 2000](#); [Benson \*et al.\* 2002](#)). It is the first time ever that galaxies impact so dramatically the global gas properties of the universe.

Several current and upcoming observations will explore the EoR with unprecedented levels of detail. The ongoing and upcoming observations of the 21-cm signal from neutral hydrogen by the Low-Frequency Array (LOFAR) and in future the Square Kilometre

Array (SKA), will explore the geometry and timing of reionization. The James Webb Space Telescope (JWST) will directly observe galaxies in the EoR to an unprecedented depth and will likely be able to constrain the sources of reionization.

Currently, there are two major outstanding questions regarding the nature of reionization. Firstly, which sources dominate the emissivity of ionizing radiation? During the EoR, active galactic nuclei and galaxies more luminous than the Milky Way are likely too rare to provide the required photon budget. Fainter galaxies are likely much more numerous, however observationally it is challenging to determine the luminosity function at such faint levels (see e.g. Sharma *et al.* 2016). In either case, the fraction of photons that escape from their natal galaxy is uncertain.

Secondly, what are the sinks of ionizing photons and how do they evolve? Each ionizing photon can ionize one neutral hydrogen atom, however the hydrogen ion can recombine again. Therefore, all sources combined need to emit more than one ionizing photon per hydrogen atom to complete reionization. The volume-averaged recombination rate per unit volume can be written as

$$\left\langle \frac{dn_{\text{HI}}}{dt} \right\rangle_{\text{rec}} = \langle \alpha_r n_e n_{\text{HII}} \rangle = c_l \alpha_r \langle n_{\text{H}} \rangle^2 \equiv c_l \frac{\langle n_{\text{H}} \rangle}{\tau_r}. \quad (1.1)$$

Here,  $n_e \approx 1.08 n_{\text{HII}}$  is the electron density, with the factor 1.08 applicable if Helium is singly ionized,  $\alpha_r$  is the recombination coefficient, and  $\tau_r$  a characteristic recombination time. The factor  $c_l > 1$  is usually called the ‘clumping factor’: it quantifies how much the recombination rate in a clumpy IGM is higher compared to that in a uniform IGM. Using the value of the case-B recombination rate at a temperature of  $T = 2.2 \times 10^4 \text{K}$  for the recombination coefficient, the product  $\tau_r(z) H(z) \approx ((1 + 6.2)/(1 + z))^{3/2}$  for the values of the cosmological parameters from Planck Collaboration (2014), where  $H(z)$  is the Hubble constant. This shows that for  $c_l \approx 1$ , recombinations cease to be important below a redshift  $z \sim 6$  in the uniform IGM.

However, recombinations are enhanced in regions of higher density, such as the filaments of the cosmic web, minihalos<sup>†</sup> and more massive halos. They increase the value of the clumping factor  $c_l$  and hence also the number of photons per baryon required to reionize the universe. In this work, we investigate the evolution of  $c_l$  due to photoevaporation of minihalos, using high resolution radiation-hydrodynamic simulations that resolve even the smallest minihalos. We provide an overview of our simulations and methodology in the next section. We then present our results, discussions, and a future outlook.

## 2. Overview of our method

The IGM’s temperature is coupled to that of the CMB by residual electrons up to a redshift of  $\approx 137$ , after which the gas cools adiabatically (see e.g. Peebles 1993). The value of the Jeans mass,

$$M_J = \left( \frac{5k_{\text{B}}T}{G\mu m_{\text{H}}} \right)^{3/2} \left( \frac{3}{4\pi\rho} \right)^{1/2}, \quad (2.1)$$

is then  $\sim 4 \times 10^3 \left( \frac{1+z}{9} \right)^{3/2} M_{\odot}$  before reionization, where  $z$  is the reionization redshift. Here,  $\rho$  is the total density (baryons plus dark matter), and the numerical values assume a temperature  $T = 1.6 \text{K}$ , and mean molecular weight,  $\mu = 1.23$ , as is appropriate for

<sup>†</sup> Minihalos are the halos that can retain baryons but cannot undergo atomic cooling due to their weak gravitational potential.

a neutral, primordial gas. Minihalos with mass larger than  $M_J$  will contribute to the clumping factor  $c_l$  and need to be resolved numerically ‡.

Photoheating during reionization increases the temperature rapidly to a value of  $T_r \approx \epsilon_\gamma / (3k_B) = 2.2 \times 10^4 (\epsilon_\gamma / 6.33 \text{ eV}) \text{K}$ , where  $\epsilon_\gamma$  is the mean energy of the ionizing photons; the numerical value assumes that the ionizing photons are emitted by hot stars with effective temperature  $10^5 \text{K}$  (see e.g. Chan *et al.* 2021). Halos with virial temperature below  $T_r$  or, equivalently, virial mass below

$$M_{\text{vir}} \lesssim 10^9 M_\odot \left( \frac{9}{1+z} \right)^{3/2}, \quad (2.2)$$

will lose a significant fraction of their baryons through photoevaporation (Okamoto Gao & Theuns 2008), which decreases  $c_l$ . We aim to simulate the photoevaporation of these minihalos and other small-scale structures numerically.

Accurately modelling the evolution of  $c_l$  requires high mass resolution to resolve halos with mass  $M_J$ . Emberson, Thomas & Alvarez (2013) found that the dark matter particle mass,  $m_{\text{dm}}$ , should not exceed  $100 M_\odot$ , for the simulations to converge. Photoevaporation significantly reduces  $c_l$ , so radiation hydrodynamics is necessary (Park *et al.* 2016; D’Aloisio *et al.* 2020). Finally, Emberson, Thomas & Alvarez (2013) claims that the simulation volume needs to be at least 1 cMpc (the “c” stands for comoving) on a side to account for sample variance.

To fulfil these requirements, we set up a high-resolution radiation-hydrodynamics cosmological simulation at high redshift. We adopt the following cosmological parameters:  $h = 0.678$ ,  $\Omega_m = 0.307$ ,  $\Omega_\Lambda = 0.693$ , and  $\Omega_b = 0.0455$ . We generate initial conditions using MUSIC (Hahn & Abel 2011). Our cubic simulation volume has a side-length,  $l_{\text{box}} = 800 \text{ ckpc}$ , and it is filled with  $512^3$  gas and dark matter particles ( $m_{\text{DM}} = 100 M_\odot$ ). Runs are performed with SWIFT (Schaller *et al.* 2016) to which we added the SPH-MIRT radiation hydrodynamics module (Chan *et al.* 2021). We use the grey approximation for the ionization cross-section, adopt the on-the-spot approximation for recombination, and use the optically-thin approximation in the calculation of the photoheating. We reduce the speed of light for computational efficiency, decreasing  $c$  by a factor of 10 at the mean density, verifying that this does not impact our results. The detailed methodology and tests will be presented elsewhere (Chan *et al.*, in prep.).

We set the redshift of reionization to  $z_r = 8$ . For redshifts  $\leq z_r$ , we inject plane-parallel radiation from two opposite sides of the cubic volume with a blackbody spectrum of temperature  $10^5 \text{K}$ . The simulation follows the propagation of the two ionization fronts through the simulated volume, calculating in detail shadowing and photoevaporation of gas in halos.

### 3. Preliminary Results

We performed simulations with two different values of the imposed photoionization rate at the edges,  $\Gamma_{-12} = 0.03$  and  $\Gamma_{-12} = 0.3$ , where  $\Gamma_{-12}$  is the photo-ionization rate in units of  $10^{-12} \text{s}^{-1}$ ; these values bracket those used by D’Aloisio *et al.* (2018). The left panel of Fig. 1 shows the dark matter and neutral gas structures at  $z = 8$  for the higher value of  $\Gamma_{-12}$ . At the left and right edges, the gas is highly ionized, in the middle of the volume, the gas is still neutral. Island of neutral gas in the highly ionized IGM correspond to dense structures with short recombination times. These include the filamentary structures of the cosmic web as well as gas in halos. The latter are visible as small yellow dots in the

‡ Pre-reionization X-ray sources can heat the IGM, boost the Jeans mass above Eq. 2.1, and reduce the IGM clumping. However, Eq. 2.1 still represents the minimum possible Jeans mass of the IGM, especially given that pre-reionization X-ray sources are highly uncertain.

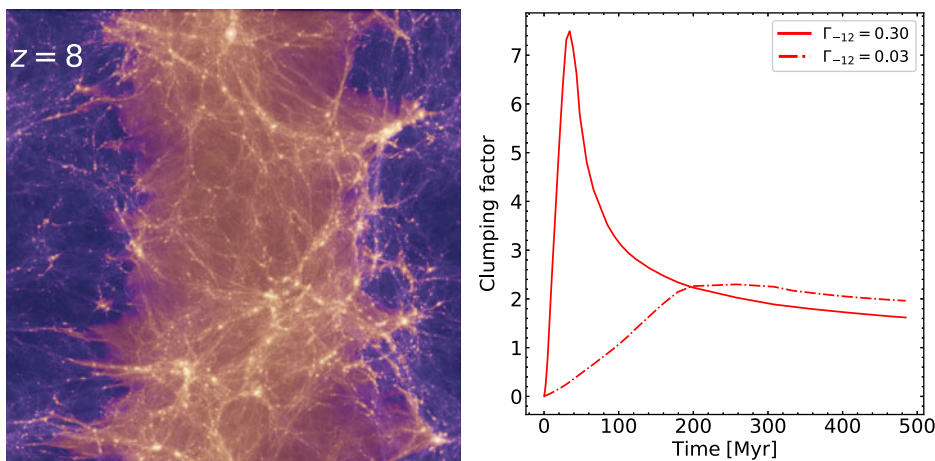


**Figure 1.** *Left panel:* A projection of neutral gas (yellow) blended with dark matter (background) in a simulation with  $\Gamma = 0.3 \times 10^{-12} \text{s}^{-1}$ ; *Right panel:* Evolution of the clumping factor,  $c_l$ , in our simulations since the onset of reionization with different values of  $\Gamma_{-12}$ , as indicated in the legend.

panel. The intervening density structures deform the initially flat ionization front into a corrugated sheet.

The right panel of Fig. 1 shows the evolution of  $c_l$  for the two choices of photo-ionization rate. Initially, the ionized gas density,  $n_{\text{HII}}$ , and the clumping factor,  $c_l$ , both increase as the ionization front traverses the volume. The clumping factor is larger for higher values of  $\Gamma_{-12}$ . As the IGM is ironed out by photoheating,  $c_l$  decreases again. Our results agree qualitatively with those from Park *et al.* (2016) and D’Aloisio *et al.* (2020).

#### 4. Discussions and Conclusion

The evolution of the clumping factor is a crucial ingredient of the physics of reionization. We find that the inhomogeneous IGM can hinder the progress of reionization by increasing the clumping factor,  $c_l$ . For the first  $\sim 100$  Myrs after the passage of an ionization front,  $c_l$  may be increased by up to a factor of 10 compared to a homogeneous IGM<sup>†</sup>. The clumping factor is even larger for higher values of the photoionization rate and/or lower redshift of reionization (Chan *et al.* in prep.). These results are consistent with previous findings, e.g. Park *et al.* (2016) and D’Aloisio *et al.* (2020). However, our values for  $c_l$  are smaller than found in studies that neglect radiation-hydrodynamic effects, such as those of e.g. Emberson, Thomas & Alvarez (2013). The hydrodynamic response of ionizing photons can reduce  $c_l$  in the IGM within a few tens of Myrs. We find that it takes only  $\sim 1$  extra photon to ionize the majority of the clumpy IGM, as compared to a homogeneous universe.

The small-scale structure of the IGM also affects the IGM opacity. Becker *et al.* (2021) present evidence for a rapid evolution of the mean free path of ionizing photons,  $\lambda_{\text{MF}}$ , between  $z = 6$  and  $z = 5$ . Cain *et al.* (2021) and Davies *et al.* (2021) argued that this implies a significant evolution of the mean value of  $\Gamma_{-12}$ . It would be interesting to study the correlation between  $c_l$ ,  $\lambda_{\text{MF}}$  and  $\bar{\Gamma}_{-12}$ . We are currently performing a suite of high-resolution radiation-hydrodynamic cosmological simulation that span different box sizes, redshifts of reionization and imposed photoionization rates (Chan *et al.* in prep.).

<sup>†</sup> See, e.g. Shapiro & Giroux (1987); Ciardi *et al.* (2006), for the effect of clumping on cosmological ionization front.

We will use this suite to investigate the impact of minihalos on reionization and the evolution of  $\lambda_{\text{MF}}$ .

## 5. Acknowledgement

This work was supported by the Science and Technology Facilities Council (STFC) astronomy consolidated grant ST/P000541/1 and ST/T000244/1. We acknowledge support from the European Research Council through ERC Advanced Investigator grant, DMIDAS [GA 786910] to CSF. ABL acknowledges support by the European Research Council (ERC) under the European Union's Horizon 2020 research and innovation program (GA 757535) and UNIMIB's Fondo di Ateneo Quota Competitiva (project 2020-ATESP-0133). This work used the DiRAC@Durham facility managed by the Institute for Computational Cosmology on behalf of the STFC DiRAC HPC Facility ([www.dirac.ac.uk](http://www.dirac.ac.uk)). The equipment was funded by BEIS capital funding via STFC capital grants ST/K00042X/1, ST/P002293/1, ST/R002371/1 and ST/S002502/1, Durham University and STFC operations grant ST/R000832/1. DiRAC is part of the National e-Infrastructure. This work made use of SPHViewer ([Benitez-Llambay 2015](#)).

## References

- Becker G. D., D'Aloisio A., Christenson H. M., Zhu Y., Worseck G. & Bolton J. S. 2021, *MNRAS*, 508, 1853
- Benitez-Llambay A. 2015, py-sphviewer: Py-SPHViewerv1.0.0, doi:10.5281/zenodo.21703
- A. J. Benson, C. S. Frenk, C. G. Lacey, C. M. Baugh & S. Cole 2002, *MNRAS*, 333, 177
- Bullock J. S., Kravtsov A. V. & Weinberg D. H. 2000, *ApJ*, 539, 517
- Cain C., D'Aloisio A., Gangolli N. & Becker G. D. 2021, *ApJL*, 917, L37
- Chan T. K., Theuns T., Bower R. & Frenk C. 2021, *MNRAS*, 505, 5784
- Ciardi B., Scannapieco E., Stoehr F., Ferrara A., Iliev I. T., & Shapiro P. R. 2006, *MNRAS*, 366, 689
- D'Aloisio A., McQuinn M., Davies F. B. & Furlanetto S. R., 2018, *MNRAS*, 473, 560
- D'Aloisio A., McQuinn M., Trac H., Cain C. & Mesinger A. 2020, *ApJ*, 898, 149
- Davies F. B., Bosman S. E. I., Furlanetto S. R., Becker G. D. & D'Aloisio A. 2021, *ApJL*, 918, L35
- Efstathiou, G. 1992, *MNRAS*, 256, 43P
- Emberson J. D., Thomas R. M. & Alvarez M. A., 2013, *ApJ*, 763, 146
- Moore B., Ghigna S., Governato F., Lake G., Quinn T., Stadel J. & Tozzi P. 2000, *ApJL*, 524, L19
- Hahn O. & Abel T. 2011, *MNRAS*, 415, 2101
- Haiman Z., Abel T. & Madau P. 2001, *ApJ*, 551, 599
- Okamoto T., Gao L. & Theuns T., 2008, *MNRAS*, 390, 920
- Park H., Shapiro P. R., Choi J.-h., Yoshida N., Hirano S. & Ahn K. 2016, *ApJ*, 831, 86
- Peebles, P. J. E. 1993, Principles of Physical Cosmology by P.J.E. Peebles. Princeton University Press, 1993. ISBN: 978-0-691-01933-8
- Planck Collaboration, Ade, P. A. R., Aghanim, N., et al. 2014, *A&A*, 571, A16
- Robertson, B. E. 2021, *arXiv*, 2110.13160
- Schaller M., Gonnet P., Chalk A. B. G. & Draper P. W. 2016, *arXiv*, 1606.02738
- Shapiro P. R. & Giroux M. L. 1987, *ApJL*, 321, L107
- Sharma M., Theuns T., Frenk C., Bower R., Crain R., Schaller M., Schaye J., 2016, *MNRAS*, 458, L94
- Theuns T. 2021, *MNRAS*, 500, 2741

## Discussion

HUI LI: Hi TK. Nice to see you again. I have a question about the clumping factor. I totally agree with you that with high resolution you can resolve more clumpiness for

the simulation and then change the recombination rate. But my question is at which resolution we can fully resolve this. This is really a desperate problem, because the higher the resolution the more clumpiness you will observe in the simulation.

TSANG KEUNG CHAN: That is a very good question. There were some studies a few years ago that did a very high resolution and found that convergence of the clumpiness is around the mass resolution we use here, so we take this mass resolution. But we have radiation hydrodynamics. They post-processed the simulations with radiative transfer, so they can run faster. However, they do not consider, e.g., radiative heating, so they overestimated the clumpiness. But even in that case, they also found convergence at this mass scale. Thus, we should be able to resolve the clumping factor at this resolution.

CHIA YU HU: My question is also related to the clumping factor. Is the clumping factor in your clumping factor defined globally? Or do you use a scale to define that when you do the averaging?

TSANG KEUNG CHAN: At least in our study and also other paper, we define the clumping factor in the whole box. This will depend on the box size you choose because they have different structures.

CHIA YU HU: But it could be that the small scale clumping doesn't play a role in a large scale clumping.

TSANG KEUNG CHAN: It depends on how large the clumping factor is. We find the clumping factor can be up to 10 or 20. If there are also many minihalos in large boxes, then supposedly they should also contribute significantly to the clumping factor.